LAWRENCE
LIVERMORE
NATIONAL
LABORATORY

LLNL-CONF-694928

Charaterization of x-ray framing cameras for the National Ignition Facility using single photon pulse height

J. P. Holder, L. R. Benedetti , D. K. Bradley

June 14, 2016

21st Topical Conference on High-Temperature Plasma Diagnostics (HTPD 2016)
Madison, WI, United States
June 5, 2016 through June 8, 2016

Disclaimer

Characterization of x-ray framing cameras for the National Ignition Facility using single photon pulse height[a)]

J. P. Holder,[1,b] L. R. Benedetti,[1] and D. K. Bradley[1,]

[1]*Lawrence Livermore National Laboratory, Livermore, California, 94550, USA*

(Presented XXXXX; received XXXXX; accepted XXXXX; published online XXXXX)

Single hit pulse height analysis is applied to microstripline microchannel plate (MCP) based x-ray framing cameras to quantify signal and noise processes. Image formation statistics (gain and noise) are assessed in both DC calibration mode and gated operation to better quantify signal and noise in x-ray framing cameras.

I. INTRODUCTION

The Gated X-ray Detector (GXD)[1,2] and the Hardened Gated X-ray Detector (HGXD)[3] are used to collect most of the time-resolved x-ray images at the National Ignition Facility (NIF). The basic operation of these microstripline micro-channel plate (MCP) based x-ray framing cameras[4] is understood but the accumulation of small variations in instrument build lead to variations of ~5X in mean instrument response that are not accurately predicted by routine characterization techniques.[6,7].

In this paper, we use single hit pulse height analysis as a complement to other methods to calibrate the gain of these cameras. We find that we can use the pulse height analysis of images collected in DC operation to validate an exponential distribution of gain (and noise) and to determine quantum efficiency (QE(hν)). .

In addition, we applied pulse-height analysis to pulsed data. In some operating modes a large noise contributor is the gain process of the MCP[8]. Since gain gating is used, both the response and the noise in that response vary in both time and position on the detector. This analysis was thus applied as an attempt to understand the interplay of the fundamental processes governing gain and noise in normal gated framing camera operation.

These techniques may allow smaller pulsed x-ray and laser generated x-ray sources to be used to better predict performance on NIF.[6]

II. DC OPERATION

The response of the GXD to an x-ray is understood to be the product of: QE (probability of amplification), MCP gain (may include secondary electron yield) and conversion to digitized signal[9]. When a photon interacts with the microchannel plate, secondary electrons are created. If a secondary electron reaches a channel, it is accelerated along the channel by the MCP voltage, creating additional electrons with each collision. The aspect ratio of the channel (together with the voltage) leads to on average 20 collisions (for GXD), creating a gain power law of voltage with exponent ~10. The electrons leave the micro-channel and are accelerated across a small gap to a phosphor deposited on a fiber optic block, generating light that is collected by the fibers in the block and coupled to a CCD camera. (Here we present data only from GXD, and we therefore ignore the additional conversion and digitization steps associated with film-based cameras, e.g. HGXD.)

The image of the cloud of electrons from a single pore (and single initial photon) spans multiple CCD pixels, forming the core of the point spread function for the instrument. A single detected x-ray photon thus results in a Gaussian like "blob" or "star" on the CCD (see Figure 1c). We call the sum of these signals – spread over neighboring pixels but due to a single initial photon – the single photon pulse height or the detector gain, G. (CCD counts/event)

The probability density function for MCP amplification is a negative exponential: the probability of observing a given G_{det} is $P(G_{det}) = (1/G_{ave})\exp(-G_{det}/G_{ave})$. Consequently, MCPs operating in the linear regime produce single event detection gain pulse heights that essentially follow a negative exponential probability distribution (details and deviations in references).[9,10,11]The low-signal end of the distribution is difficult to differentiate from noise, but a semilog plot of the histogram of pulse heights can be linearly fit, and the inverse of the slope of that line is then used to estimate the underlying average gain G_{ave}, without bias due to missing events below the noise threshold. For mean detector gain G_{ave}, the standard deviation of samples from an exponential distribution is also G_{ave}. Thus, in a well-sampled distribution, the slope and intercept on a semi-log plot and the mean and standard deviation of all pulse heights will all lead to the same G_{ave}. By identifying single detected events QE be factored out of the response, and the product of MCP gain and conversion to digitized signal is determined directly.

The statistical distribution of events may be observed by reducing the photon fluence (flux x time) to the MCP until individual events are well separated. Figure 1a shows such an image, a short shuttered exposure on a filtered DC x-ray source (~8.2keV average photon energy) acquired with GXD1 operating in DC mode (MCP at -750V DC and phosphor at 3kV)[11,12] Figure 1b zooms in to show overlays of 12 pixel diameter circles around identified "events". Figure 1c examines at a single event. Figure 1d shows the summing of counts in the event over

[a)]Contributed paper published as part of the Proceedings of the 21st Topical Conference on High-Temperature Plasma Diagnostics (HTPD 2016) in Madison, Wisconsin, USA.

[b)]Author to whom correspondence should be addressed: holder4@llnl.gov.

increasing radii. The choice of radius is important because counting over too small an area will miss real signal, but counting over too large an area will add value from local background noise. Using the surrounding pixels as a local background, this event pulse height is 3672 counts, and it fits within a radius of 6 pixels. This aperture and correction method is used for all events. Systematic studies of image processing, event selection, rejection and integration are still needed for error analysis.

A histogram of pulse heights taken from the first strip (top in image Figure 1a) is shown in Figure 2a with semi-log linear fits. From the first slope the average single event detector gain is estimated to be ~2130 counts. This is consistent with the mean value of the observed pulse heights of 2450 counts and standard deviation of 2320 counts. This is the gain due to a single x-ray photon, not necessarily a single photoelectron, as one high-energy x-ray may produce multiple photoelectrons. The analysis of smaller regions finds the number of events detected in each of the four strips and in gain across each strip to be nearly uniform. However, a small difference in detector gain (~15%) is seen between different strips. Some of this difference may be due to the separate power supplies used for each strip, but the observation of a gradient in gain from top to bottom suggests other causes, such as pore bias, MCP-phosphor gap wedging, or coating and coupling non-uniformities.

A longer duration exposure in which events are accumulated and superimposed until the image intensity is smooth can be used to determine an average response of the detector. Photon flux to the detector is measured with a calibrated diode allowing an absolute measurement of (DC) response (86 CCD counts per incident photon). Together with the average gain per amplified photon, this allows an estimate of quantum efficiency of 4±1% [16].

III. GATED OPERATION

In gated operation, the same basic x-ray amplification process happens, except that the electric fields in the channel plate are changing rapidly, and the time of flight between collisions can be significant[4]. At a chosen time, ~-1kV 200ps FWHM Gaussian-like electrical pulse is launched into each strip, acting as a microstripline transmission line, propagating right to left (as viewed in our images, through the phosphor) with velocity of ~150 mm/ns (for GXD1 MCP) , so the length of a strip maps to ~250ps. Any position on the microstrip sees a time varying voltage, and any x-ray generated electrons will respond to voltages that vary as they transit down the pore. Only photoelectrons made early enough to be accelerated down the entire channel get substantial MCP gain, so for short pulses the caught and amplified photoelectrons mostly arrive before the peak of the electrical gating pulse.

The effective gain gating function depends on the shape of the electrical pulse. The gating gain shape and propagation along the microstripline is measured with a short pulse UV laser[5,7]. Also observed is that the propagation of the high voltage pulse is lossy, so that there is usually a factor of ~3 less MCP gain at the exit of the strip than at the entrance, the "gain droop". To adjust gain, a DC bias voltage is added to the pulsed voltage. Confounding effects are reflections, stray electrons and crosstalk.[5] Also because higher phosphor voltages can be sustained over short sub-millisecond durations, the phosphor voltage is increased to 5kV for the electrons exiting the MCP, producing for the GXD a 2X increase in light output relative to the 3kV DC case.

Individual events were observed in gated operation using the flux produced by 1TW of NIF laser focused to an Au sphere[6]. The GXD1 was configured with a 100V bias on all microstrips, and operated with a 5kV pulsed phosphor voltage. The gating times for each strip had greater than 500ps relative delays, minimizing the expectation of crosstalk-induced gain. The image, filtered for 8-9 keV photons, had distinguishable events that were processed in the same way as the DC x-ray image. The number of photons counted in each strip varied (presumably from the source changing in time). Figure2b is a histogram of events from the first strip. When fitted as if this were a DC image, we can use the first slope as a weighted measure of average gain. Using this measure of "gain", the ratio of gain between strips is similar to ratios measured with a short pulse UV laser. By looking at sub-regions, the "gain" on the early time part of a strip is larger than the "gain" on the right, showing gain droop.

A good estimate of the average pulse height at the peak of the gating pulse in the center of strip 1 is from Figure2b and the model guidance is 5400 ccd counts/photon and an average value of 2700 counts/photon, with the caveat that the DC data also had a second component partially due to the assignment of multiple photon hits to an event. Scaling up the DC results with phosphor voltage ~4250 counts/photon. A larger difference was expected from the ~100V greater MCP voltage in the gated case. One factor may be our accounting of photoelectron yield. More data is needed to validate the models and measurements used.

IV. SIMPLE MODEL OF GATED IMAGE

Extracted peak and gate time average values from pulse height spectra of small areas along each strip are desired. In a preliminary effort to relate the pulsed x-ray measurement to desired quantities, a very simple model was created. In the first demonstration of the model we simulate a short pulse of events hitting a similar size detector with a non-drooping 100ps FWHM gain pulse is at the center of the detector, scaling pulse propagation as in the real detector. We set the peak gain of the gating pulse to be 1000 per perfectly detected event. Sample events are randomly assigned to positions on the detector. Those events then acquire an average gain related to that position (and time). A pulse height is randomly assigned to that event, scaled to the assigned average gain. Figure 3a is a histogram of all the pulse heights simulated including those with values less than 1. The manually selected linear fits show that the second slope fitting process "finds" the peak gain. Note in this no droop case this histogram also represents of the pulse height distribution a single point on the detector over the (most of) the gating time.

Figure 3b is a histogram of a second simulation where the gain pulse is propagated across the detector. We randomly select the times of each event from a uniform random distribution form range 1000 ps centered on the time that the gating pulse is in the center of the detector. A linear gain droop was also simulated, with the peak gain of 1500 at the entrance, 1000 in the center and 500 at the gate pulse exit. There are more events in the low gain region. Again, using the same fit section regions, the second slope has "found" an "average" value of the peak. Better fitting and more parameter sensitives need to be explored.

V. CONCLUSIONS

The results we have reported are preliminary, and specifically we need to apply these analysis techniques to additional data to have confidence in the accuracy and uncertainty of our conclusions. Still we find pulse height counting to be a useful tool that allows the separation of gain from detection efficiency. This leads to an improved quantitative understanding of framing camera signals and noise. More robust tools and processes are being explored for routine use in with DC x-ray sources. A pulse height gate profile in the UV would be a good way to determine if the pulse height distribution is still exponential-like though out a gate pulse. The results from the gated data and simple model suggest that other x-ray sources could be used to understand and validate a transfer of our current DC x-ray and gated UV instrument measurement to behavior for gated x-ray instruments used on NIF experiments.

ACKNOWLEDGMENTS

This work was performed under the auspices of the U.S. Department of Energy by Lawrence Livermore National Laboratory under Contract DE-AC52-07NA27344. Lawrence Livermore National Security, LLC. LLNL-CONF-694928.

DC x-ray measurements acquired by National Security Technologies, Livermore Operations for (deliverable under DOE Prime Contract No. DE-AC52-06NA25946).

[1]J. A. Oertel, R. Aragonez, T. Archuleta, C. Barnes, L. Casper, V. Fatherley, T. Heinrichs, R. King, D. Landers, F. Lopez, P. Sanchez, G. Sandoval, L. Schrank, P. Walsh, P. Bell, M. Brown, R. Costa, J. Holder, S. Montelongo, and N. Pederson, "Gated x-ray detector for the National Ignition Facility," Rev. Sci. Instrum. **77**, 10E308 (2006).

[2] J.R. Kimbrough, P.M. Bell, D.K. Bradley, J.P. Holder, D.K. Kalantar, A.G. MacPhee and S. Telford, "Standard design for National Ignition Facility x-ray streak and framing cameras," Rev. Sci. Instrum. **81**, 10E530(2010).

[3] D.R. Hargrove, J.P. Holder, N. Izumi, L.R. Benedetti, J. Kimbrough P.M. Bell and S. Glenn, "Improvements to a MCP based high speed x-ray framing camera to have increased robustness in a high neutron environment,", Proc. SPIE **9211**, 92110D (2014).

[4]J.D. Kilkenny, "High Speed Proximity Focused X-ray Cameras," Lasers and Partilce Beams, 9(1), 49(1991).

[5] L. R. Benedetti, J. P. Holder, M. Perkins, C. G. Brown, C. S. Anderson, F.V. Allen, and R. B. Petre, D. Hargrove, S. M. Glenn, N. Simanovskaia, D. K. Bradley, and Bell, P., "Advances in x-ray framing cameras at the National Ignition Facility to improve quantitative precision in x-ray imaging," Review of Scientific Instruments, 87, 023511 (2016)

[6]S.F. Khan, L.R. Benedetti, D.R. Hargrove, S.M. Glenn, N. Simanovskaia, J.P. Holder, M.A. Barrios, D. Hahn, S.R. Nagel, P.M. Bell, and D. K. Bradley, "Methods for characterizing x-ray detectors for use at the National Ignition Facility,' Rev. of Sci. Instrum. **83**, 10E118 (2012).

[7]L. R. Benedettil, C. Trosseille, J. P. Holder, K. Piston, D. Hargrove, D. K. Bradley, P. Bell, J.Raimbourg, M. Prat, L. A. Pickworth, and S. F. Khan, "A Comparison of Flat Fielding" Techniques for X-ray Framing Cameras," (to appear in these proceedings)

[8]G. A. Kyrala, J. Oertel, T. Archuletaa and J. Holder, "Gain Spectrum in Gated X-ray MCPs", Proc. of SPIE **7448,** 74480S (2009). (Note high gain CCD settings used).

[9]J.L. Wiza, "Microchannel Plate Detectors",NIM**162**,587(1979).

[10] K. W Dolan and J. Chang," Microchannel Plate Response to Hard X-rays", *Proc. SPIE* **0106**, 178(1977).

[10]BURLE Corp "Photmultiplier Handbook", TP-136, Appendix G (1980)

[11]Manson Model 5, Austin Instruments, Inc. 10 Temple St., Reading MA 01867-2830

[12]M. J. Haugh and M. Schneider (2011). Quantitative Measurements of X-Ray Intensity, Photodiodes - Communications, Bio-Sensings, Measurements and High-Energy Physics, Jin-Wei Shi (Ed.),: http://www.intechopen.com/books/photodiodes-communications-bio-sensings-measurements-and-high-energy-physics/quantitative-measurements-of-x-ray-intensity

[13]Rasband, W.S., ImageJ, U. S. National Institutes of Health, Bethesda, Maryland, USA, http://imagej.nih.gov/ij/, 1997-2016.

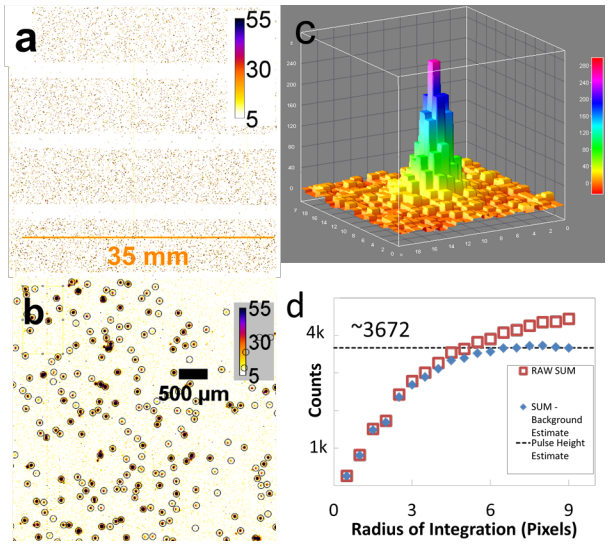

Figure 1: Single events observed in DC operations. a) entire camera image b) zoom c) a single event d) sum of the event as a function of radius from found peak. Red squares indicate total signal within radius, and blue diamonds indicate total signal minus a locally-determined average background. ImageJ was used to process images[13].

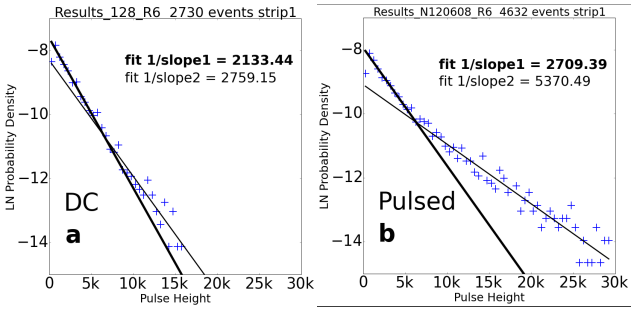

Figure 2: Semi-log histograms of measured event pulse heights from images taken with strip1 of GXD1 a) DC X-ray and b) is Pulsed Gated on NIF experiment. A 500 count bin width was used. Lines are unweighted fits to the same sections of each histogram.

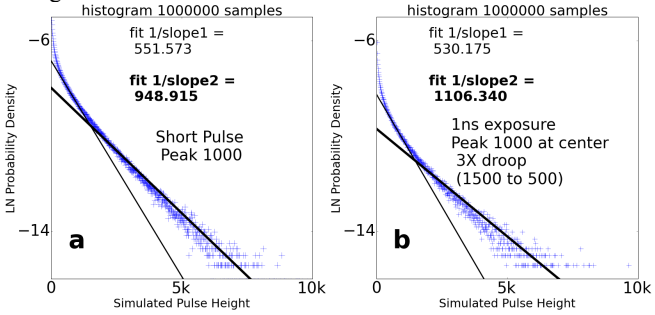

Figure 3: Semi-log histograms of simulated event pulse heights for a) simulating short pulse laser excitation of an ideal 100ps FWHM gated camera and b) simulating a flat field shot with gain transiting the simulated camera with a factor of 3 droop.